Modulation of membrane permeability by carbon dioxide

Hong Zhang, Xueguang Shao, Francois Dehez, Wensheng Cai, Christophe Chipot

Modulation of Membrane Permeability by Carbon Dioxide

Hong Zhang,[1] Xueguang Shao,[1, 2, 3] François Dehez,[4, 5] Wensheng Cai,[*, 1, 3] and Christophe Chipot[*, 4, 5, 6]

Correspondence to: Christophe Chipot (chipot@ks.uiuc.edu); Wensheng Cai (wscai@nankai.edu.cn)

[1] *Research Center for Analytical Sciences, College of Chemistry, Nankai University, Tianjin Key Laboratory of Biosensing and Molecular Recognition, Tianjin 300071, China.*
[2] *State Key Laboratory of Medicinal Chemical Biology, Tianjin 300071, China*
[3] *Collaborative Innovation Center of Chemical Science and Engineering, Tianjin, 300071, China*
[4] *Laboratoire International Associé CNRS and University of Illinois at Urbana−Champaign, Vandœuvre−lès−Nancy F-54506, France*
[5] *LPCT, UMR 7019 Université de Lorraine CNRS, Vandœuvre−lès−Nancy F-54500, France*
[6] *Department of Physics, University of Illinois at Urbana−Champaign, Urbana, Illinois 61801, United States*

ABSTRACT

Promoting drug delivery across the biological membrane is a common strategy to improve bioavailability. Inspired by the observation that alcoholic carbonated beverages can increase the absorption rate of ethanol, we speculate that carbon dioxide (CO_2) molecules could also enhance membrane permeability to drugs. In the present work, we have investigated the effect of CO_2 on the permeability of a model membrane formed by 1-palmitoyl-2-oleoyl-sn-glycero-3-phosphocholine (POPC) lipids to three drug-like molecules, namely, ethanol, 2',3'-dideoxyadenosine (DDA), and trimethoprim. The free-energy and fractional-diffusivity profiles underlying membrane translocation were obtained from μs-timescale simulations and combined in the framework of the fractional solubility-diffusion model. We find that addition of CO_2 in the lipid environment results in an increase of the membrane permeability to the three substrates. Further analysis of the permeation events reveals that CO_2 expands and loosens the membrane, which, in turn, facilitates permeation of the drug-like molecules.

Introduction

Although many new drugs have been designed and synthesized over the past decades,[1] not all drugs are utilized effectively.[2, 3] There are many factors affect the drug bioavailability, for example, its solubility, permeability, absorption and cytotoxicity.[4, 5] Poor bioavailability of drugs can increase the medical cost, on the one hand, and decrease the recovery rate of patients, on the other hand.[3] Increasing the drug bioavailability is still one of the main challenges in medicine field.[6] Recently, various approaches have been studied to improve the pharmacokinetic and physicochemical properties of drugs to increase their bioavailability.[6, 7] One strategy relies on the modification of drug molecules to improve their solubility and effects,[8] which costs a lot of time before clinical application. One approach is to use drug carriers, for example, enteric coating, one of the traditional drug delivery approaches applied to oral drugs.[9, 10] Recently, many new-type drug carriers have been designed to target the tumor cells.[11, 12] Another strategy is to improve the penetration of drugs through membranes.

The permeability is a significant property to describe the absorption rate of drug candidates inside the body. Increasing the permeability of drug is one important strategy to enhance its bioavailability.[13] Recently, many approaches were reported to improve the membrane permeability. V. Khutoryanskiy and coworkers proposed that crown ethers can increase the permeability of ocular drugs.[14] Perkins et al. put forward that phenylalanine can enhance the membrane permeability.[15] Among these approaches, the cytotoxicity of the additives needs to be considered. Therefore, seeking a strategy with a low cytotoxicity appears to be very necessary.

Robinson and Roberts studied the effect of the mixture of ethanol and carbonated beverages on the blood ethanol level.[16] As mentioned about one hundred years ago,[17] their results indicate that the mixture of ethanol and carbonated drinks can increase the absorption rate of ethanol. The same conclusion was reached by Ridout et al. who proved that champagne is more inebriant than wine.[18] These observations prompt us to speculate that, at the microscopic level, CO_2 might affect the overall permeability of membrane cells, possibly increasing the absorption rate of any small molecule. In the present work, we disentangled the relationship between CO_2 and the membrane permeability by means of all-atom molecular-dynamics simulations. The permeation of three drug-like molecules, namely, ethanol, 2',3'-dideoxyadenosine (DDA) and trimethoprim, through a 1-palmitoyl-2-oleoyl-sn-glycero-3-phosphocholine (POPC) bilayer saturated with CO_2 was studied. To estimate accurately the membrane permeability to drugs, the solubility-diffusion model constitutes a powerful tool.[19-21] The free-energy calculations and the permeability estimations based on the fractional solubility-diffusion model were used to investigate the thermodynamics and kinetics properties of membrane permeation of these three permeants.

Methods

Molecular Models. The three-dimensional structures of the three small molecules, namely, ethanol, DDA, and trimethoprim (see Figure 1) were built. To compare with permeation in absence of CO_2, we used the same number of POPC molecules as in our previous works, namely, bilayers of 100, 128, and 128 POPC units for the ethanol,[20] DDA,[19] and trimethoprim assays, respectively. CHARMM36 force field parameters were utilized for POPC[22] whereas the three drugs were decribed by the CHARMM general force field (CGenFF).[23-25] The normal to the membrane is aligned with the z-axis. 180 CO_2 molecules were added randomly into these assays. The molecular assays were immersed into a box of ~59 × 59 – 67 × 67 $Å^2$ in the x, y-plane, extending up to 80 – 120 Å in the z direction, including 6,154 – 9,034 TIP3P[26] water molecules.

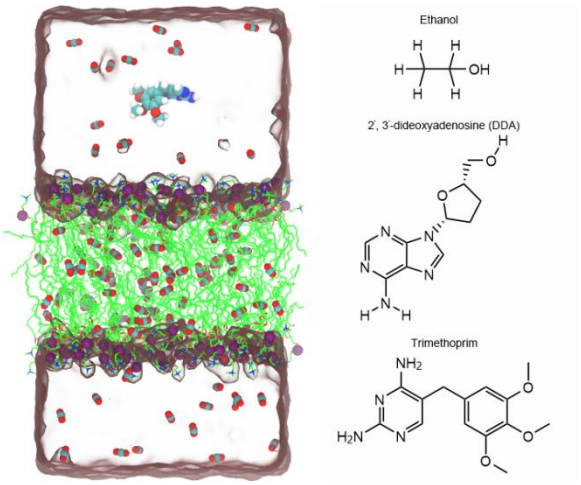

Figure 1. Structures of the three permeants studied in this work.

Simulation Protocol. All the molecular dynamics simulations were carried out by means of the program NAMD (version 2.13).[27] The Langevin piston method[28] was employed to maintain the system pressure at 1 atm. Langevin dynamics was utilized to maintain the temperature at 308 K with 1 ps^{-1} damping coefficient. Covalent chemical bonds involving hydrogen atoms were constrained to their experimental lengths for solute and water molecules, using the Rattle[29] and SETTLE algorithms,[30] respectively. The integration of motion equations was carried out using a r-RESPA multiple time-stepping algorithm with a time step of 4 and 2 fs for long- and short-range interactions, respectively.[31] Long-range electrostatic forces were evaluated by means of the particle mesh Ewald (PME) scheme.[32] A smoothed 9 Å spherical cutoff was used to truncate short-range electrostatic and van der Waals interactions. The VMD program (1.9.3) was applied to analyze and visualize the MD trajectories.[33]

Free-Energy Calculation. Before running the free-energy calculations, a 200-ns equilibrium simulation was carried out to equilibrate the CO_2 molecules. The potentials of mean force (PMF) characterizing the translocation of the small molecules across the membrane were then determined by the adaptive biasing force (ABF) algorithm.[34-36] The PMF profile describing the translocation of DDA without CO_2 was obtained from our previous study,[19] no repetitive calculations were performed in the present work. To do a fair comparison with the previous results, similar protocols were used. The transition coordinate was defined as the projection of the distance between the center of mass of the permeants and that of the phosphorus atoms of POPC molecules onto the z-axis of Cartesian space. The instantaneous force values were accrued in bins 0.1 Å. The free-energy profiles spanning from - 45 to 45 Å were broken down into nine windows, 10 – 15 Å wide with a 5 Å overlap. The free-energy profiles were eventually symmetrized with respect to center of the membrane. The sampling time for each simulation is gathered in Table S1 of the Supporting Information.

Kinetic Modeling. A variant of the Bayesian-inference scheme developed for classical diffusion[37] was used to determine the position-dependent fractional diffusivity. The details of this inference algorithm, implemented in the program DiffusionFusion,[38] were described in our previous work.[19-21] The fractional order, $\alpha(z)$, and the fractional diffusivity, $K_\alpha(z)$, were optimized. Two distinct lag times, namely, Δt = 4 ps and Δt = 16 ps, were employed. The long-tailed distributions[37] of Monte Carlo moves were presented with a value of 0.005 for $\alpha(z)$ and 3.5 $Å^2/ns^\alpha$ for $K_\alpha(z)$. ε = 0.02 $Å^{-1}$ and 20 Å/ns were used for the smoothness priors for $\alpha(z)$ and $K_\alpha(z)$, respectively. The membrane permeability was calculated by integrating over the thickness of the lipid bilayer in the framework of the fractional solubility-diffusion model of permeation.[20, 37]

Results and discussion

Free-energy Profiles of Small Molecules Across the Membrane

The free-energy profiles characterizing the translocation of three drug-like molecules across the model membrane are gathered in Figure 2. The smallest molecule among these three permeants, ethanol, yields a free-energy barrier around 2.9 kcal/mol in the pure POPC lipid bilayer while in the mixed POPC:CO_2 system, the free-energy barrier decreases to 2.2 kcal/mol. The hydrophilic DDA exhibits a much higher free-energy barrier compared to ethanol, which amounts up to ~7.5 kcal/mol at the center of the pure POPC bilayer, but reduces to 7.1 kcal/mol upon addition of CO_2. As depicted in Figure 2C, the shape of free-energy profile of trimethoprim is similar to that of DDA, presenting a free-energy barrier of 7.8 kcal/mol, in agreement with the result obtained by Sun et al.[39] The free-energy barrier decreases by 0.7 kcal/mol upon addition of CO_2 molecules. Altogether, our results clearly indicate that the

incorporation of CO_2 molecules into the POPC lipid bilayer reduces to a certain extent the free-energy barrier associated with permeation of small drugs across biological membranes.

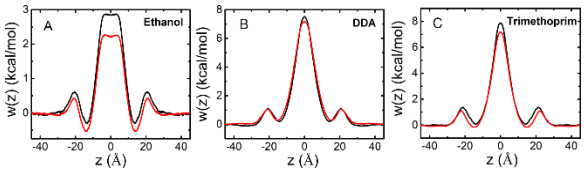

Figure 2. Free-energy profiles describing the membrane translocation of (A) ethanol, (B) DDA, and (C) trimethoprim across a pure POPC (black line) or a mixed POPC:CO_2 (red line) bilayer.

Fractional Diffusivity and Permeability of the Three Permeants Across the Membrane

In order to estimate the membrane permeability to these drug-like molecules, the fractional solubility-diffusion model of permeation was used. The fractional diffusivity, $K_\alpha(z)$, is shown in Figure 3. Though part of CO_2 molecules spread out in the aqueous phase, $K_\alpha(z)$ does not significantly change for these drugs in water phase. Interestingly enough, a slightly increase of the fractional diffusivity for the three drugs is observed in the membrane, meaning that the addition of CO_2 enhances the diffusivity of drugs in the membrane. It is worth noting that $K_\alpha(z)$ of ethanol in aqueous phase calculated herein, 240 $Å^2$/ns, differs from that determined in our previous work, 340 $Å^2$/ns.[20] It is solely a consequence of the different thermostats employed in both simulations. While Langevin dynamics was used in the present study, our previous work resorted to the Lowe-Anderson thermostat.[20] The friction term in Langevin dynamics can decrease the value of the position-dependent fractional diffusivity.[20] However, the value obtained from Langevin dynamics is much closer to the experimental one, 122 – 126 $Å^2$/ns.[40, 41]

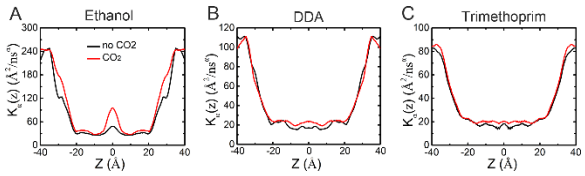

Figure 3. The fractional diffusivity for (A) ethanol, (B) DDA, and (C) trimethoprim in pure POPC and a mixed POPC:CO_2 bilayer.

The membrane permeability to the permeant was estimated from a direct integration in the framework of the fractional solubility-diffusion model of permeation. As depicted in Table 1, it is worth noting that the magnitude of experimental permeabilities differs from that inferred with simulations. This discrepancy is rooted in the difference in molecular composition of the model and the biological membranes and/or the systematic error associated with the force field. For trimethoprim, the simulation estimate is close to the permeability determined by Sun et al.[39] It appears clearly that the membrane permeabilities of POPC to the three small permeants increase upon the addition of CO_2 molecules, which may be ascribed to a modification of the membrane properties. The effect of CO_2 on the membrane is discussed in the following section. In addition, the permeability of ethanol, DDA, and trimethoprim in POPC:CO_2 mixture is around 4, 2, and 1.2 times higher than that in pure POPC, respectively. It appears that CO_2 primarily affects membrane permeabilities of small size molecules.

Table 1. Permeabilities of Each Permeant in Pure POPC and mixed POPC:CO_2 bilayers.

Permeant	Bilayer	P_m (cm s^{-1})

Ethanol	SOPC vesicles[a]	3.8×10^{-5}
Ethanol	POPC	0.26
Ethanol	POPC:CO_2	0.95
DDA	egg lecithin[b]	6.3×10^{-5}
DDA	POPC[c]	2.0×10^{-4}
DDA	POPC:CO_2	4.1×10^{-4}
Trimethoprim	egg lecithin[d]	7.2×10^{-6}
Trimethoprim	POPC	1.3×10^{-4}
Trimethoprim	POPC:CO_2	1.6×10^{-4}

[a] Experimental values obtained from Ref. [42]
[b] Experimental values obtained from Ref.[43]
[c] Theoretical estimation obtained from Chipot and coworkers.[19]
[d] Experimental values obtained from Ref.[44, 45]

The Effect of CO_2 Molecules on the Membrane Properties.

The average number of CO_2 per lipid unit is reported in Table S2 in the Supporting Information. There is ~0.8 CO_2 molecule per lipid unit for all systems. In order to examine the distribution of CO_2 molecules in the membrane, the density profiles of CO_2 along the membrane axis was plotted (see Figure 4A). Most of the CO_2 molecules permeate into the membrane on account of their hydrophobic nature. In addition, distribution of CO_2 molecules culminates in the middle of the two membrane leaflets. We calculated further the average number of CO_2 and water molecules within 2.5 Å of each atom of the three permeants along the z-axis of the mixed POPC:CO_2 system. As shown in Figure 3B, the number of CO_2 around the trimethoprim in the membrane is higher than that around DDA and ethanol. It can be rationalized by the higher hydrophobicity and the larger size of trimethoprim. As described in Figure 3C, the differences in the number of water molecules hydrating the three drugs in bulk water, can be assigned to the size of the molecules.

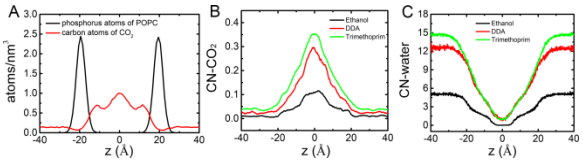

Figure 4. (A) Density profiles of POPC phosphorus and CO_2 along the axis normal to the membrane plane. Number of (B) CO_2 and (C) water molecules within 2.5 Å of the three permeants along the z-axis in the mixed POPC:CO_2 bilayer.

How do the CO_2 molecules affect the membrane properties? To answer this question, a series of analyses were performed. The phosphate-to-phosphate distance, characterizing the variation of thickness between mixed POPC:CO_2 and pure POPC membranes, was systematically determined (Figure 5A). The membrane thickness is found to increase by 1 Å upon addition of CO2, compared with the pure POPC membrane. We also analyzed the changes of the fraction mass overlap between the two leaflets (see Figure 5B), showing that insertion of CO_2 molecules decreases the leaflet interdigitation, consistently with the increase of the membrane thickness. These results support that addition of CO_2 can expand and loosen the membrane. As described in Figure 5C, the average area per lipid of pure POPC is ~68 $Å^2$, in agreement with the experimental value of 68.3 ± 1.5 $Å^2$.[46] The addition of CO_2 molecules increase this value up to ~71 $Å^2$, a situation that is consistent with an accrued membrane permeability.[47]

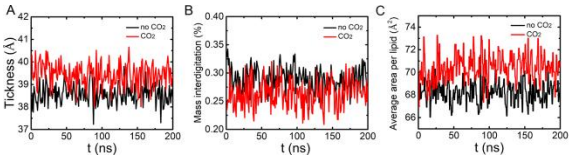

Figure 5. Evolution of (A) the phosphate-to-phosphate distance (B), the fraction mass overlap between the two leaflets, and (C) the average area per lipid during the 200-ns simulation.

Membrane fluidity is another important property affecting the membrane permeability to drugs, which can be estimated by the order parameters, S_{CD}. As shown in Figure 5, the addition of CO_2 molecules decreases the S_{CD} values of the POPC tails, which, in turn, increases the membrane fluidity. In conclusion, CO_2 molecules loosen the membrane, improving the membrane permeability and fluidity.

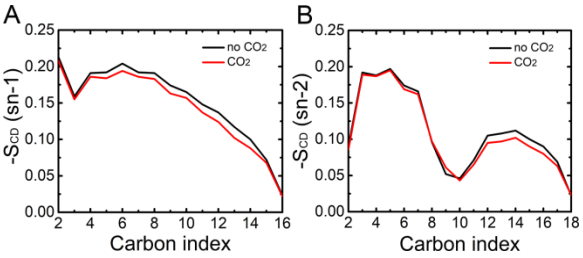

Figure 6. Average S_{CD} order parameters of POPC (A) sn-1 and (B) sn-2 tails during the 200-ns simulation.

Conclusions

In the present contribution, we investigated the effect of the CO_2 on the membrane permeability to drugs from both aspects of thermodynamics and kinetics. The permeabilities of three drug-like molecules, namely, ethanol, 2',3'-dideoxyadenosine (DDA), and trimethoprim, were examined in pure POPC and in mixed POPC:CO_2 bilayers. The free-energy profiles obtained from μs-timescale simulations indicate that the incorporation of CO_2 molecules into bilayers decreases the free-energy barrier associated with the membrane translocation of drugs. In addition, the permeabilities of three drug-like molecules increase when adding CO_2. Further analyses indicate that CO_2 molecules loosen the membrane and improve its fluidity, increasing in return its permeability to small molecules. The data reported in the present work provide an appealing view about the modulation of drug permeability by CO_2. The present theoretical framework opens the way toward understanding the effect of gas molecules on membrane properties.

Acknowledgments

This study was supported by the National Natural Science Foundation of China (21773125), and the Natural Science Foundation of Tianjin, China (18JCYBJC20500). The authors acknowledge support from the Centre National de la Recherche Scientifique through an integrated program of scientific cooperation (PICS) with China. H. Zhang gratefully acknowledges the financial support from China Scholarship Council (No. 201806200074).

Keywords: membrane permeability, CO_2, drug

(Additional Supporting Information may be found in the online version of this article.)

References and Notes

1. M. E. Noble, J. A. Endicott, L. N. Johnson, *Science* **2004**, *303*, 1800-1805.
2. G. Sliwoski, S. Kothiwale, J. Meiler, E. W. Lowe, *Pharmacol. Rev.* **2014**, *66,* 334-395.
3. J. A. DiMasi, R. W. Hansen, H. G. Grabowski, *J. Health. Econ*. **2003**, *22*, 151-185.
4. K. Tsaioun, M. Bottlaender, A. Mabondzo, BMC Neurol. **2009**.
5. J. Bowes, A. J. Brown, J. Hamon, W. Jarolimek, A. Sridhar, G. Waldron, S. Whitebread, *Nat. Rev. Drug Discovery* **2012**, *11,* 909.
6. P. Fasinu, V. Pillay, V. M. Ndesendo, L. C. du Toit, Y. E. Choonara, *Biopharm. Drug Dispos.* **2011**, *32*, 185-209.
7. R. Panchagnula, N. S. Thomas, *Int. J. Pharm.* **2000**, *201*, 131-150.
8. R. N. Gursoy, S. Benita, *Biomed. Pharmacother.* **2004**, *58*, 173-182.
9. P.-C. Ho, D. J. Saville, S. Wanwimolruk, *J. Pharm. Pharm. Sci.* **2001**, *4*, 217-227.
10. F. Eeckman, A. J. Moës, K. Amighi, *Int. J. Pharm.* **2002**, *241*, 113-125.
11. S. Zhang, Z. Chu, C. Yin, C. Zhang, G. Lin, Q. Li, *J. Am. Chem. Soc.* **2013**, *135*, 5709-5716.
12. M. M. Kamphuis, A. P. Johnston, G. K. Such, H. H. Dam, R. A. Evans, A. M. Scott, E. C. Nice, J. K. Heath, F. Caruso, *J. Am. Chem. Soc.* **2010**, *132*, 15881-15883.
13. N. D. Derle, R. Bhamber, *J. Appl. Pharm. Sci.* **2012**, *2*, 34-39.
14. P. W. Morrison, N. N. Porfiryeva, S. Chahal, I. A. Salakhov, C. n. Lacourt, I. I. Semina, R. I. Moustafine, V. V. Khutoryanskiy, Mol. Pharmaceutics **2017**, *14*, 3528-3538.
15. R. Perkins, V. Vaida, *J. Am. Chem. Soc.* **2017**, *139*, 14388-14391.
16. C. Roberts, S. Robinson, *J. Forensic. Leg. Med*. **2007**, *14*, 398-405.
17. N. Edkins, M. Murray, *J. Physiol.* **1926**, *62*, 13-16.
18. F. Ridout, S. Gould, C. Nunes, I. Hindmarch, *Alcohol Alcohol.* **2003**, *38*, 381-385.
19. C. H. Tse, J. Comer, Y. Wang, C. Chipot, *J. Chem. Theory Comput.* **2018**, *14*, 2895-2909.
20. J. Comer, K. Schulten, C. Chipot, *J. Chem. Theory Comput.* **2017**, *13*, 2523-2532.
21. C.-H. Tse, J. Comer, S. K. Sang Chu, Y. Wang, C. Chipot, *J. Chem. Theory Comput.* **2019**.
22. J. B. Klauda, R. M. Venable, J. A. Freites, J. W. O'Connor, D. J. Tobias, C. Mondragon-Ramirez, I. Vorobyov, A. D. MacKerell Jr, R. W. Pastor, *J. Phys. Chem. B* **2010**, *114*, 7830-7843.
23. K. Vanommeslaeghe, E. Hatcher, C. Acharya, S. Kundu, S. Zhong, J. Shim, E. Darian, O. Guvench, P. Lopes, I. Vorobyov, *J. Comput. Chem.* **2010**, *31*, 671-690.
24. K. Vanommeslaeghe, A. D. MacKerell Jr, *J. Chem. Inf. Model.* **2012**, *52*, 3144-3154.
25. K. Vanommeslaeghe, E. P. Raman, A. D. MacKerell Jr, *J. Chem. Inf. Model.* **2012**, *52*, 3155-3168.
26. W. L. Jorgensen, J. Chandrasekhar, J. D. Madura, R. W. Impey, M. L. Klein, *J. Chem. Phys.* **1983**, *79*, 926-935.
27. J. C. Phillips, R. Braun, W. Wang, J. Gumbart, E. Tajkhorshid, E. Villa, C. Chipot, R. D. Skeel, L. Kale, K. Schulten, *J. Comput. Chem.* **2005**, *26*, 1781-1802.
28. S. E. Feller, Y. Zhang, R. W. Pastor, B. R. Brooks, *J. Chem. Phys.* **1995**, *103*, 4613-4621.
29. H. C. Andersen, *J. Comput. Chem.* **1983**, *52*, 24-34.
30. S. Miyamoto, P. A. Kollman, *J. Comput. Chem.* **1992**, *13*, 952-962.
31. M. Tuckerman, B. J. Berne, G. J. Martyna, *J. Chem. Phys.* **1992**, *97*, 1990-2001.
32. T. Darden, D. York, L. Pedersen, *J. Chem. Phys.* **1993**, *98*, 10089-10092.

33. W. Humphrey, A. Dalke, K. Schulten, *J. Mol. Graphics* **1996**, *14*, 33-38.
34. E. Darve, A. Pohorille, *J. Chem. Phys.* **2001**, *115*, 9169-9183.
35. J. Comer, J. C. Gumbart, J. Hénin, T. Lelièvre, A. Pohorille, C. Chipot, *J. Phys. Chem. B* **2014**, *119*, 1129-1151.
36. H. Fu, X. Shao, C. Chipot, W. Cai, *J. Chem. Theory Comput.* **2016**, *12*, 3506-3513.
37. J. Comer, C. Chipot, F. D. González-Nilo, *J. Chem. Theory Comput.* **2013**, *9*, 876-882.
38. C. Chipot, J. Comer, *Sci. Rep.* **2016**, *6*, 35913.
39. R. Sun, Y. Han, J. M. Swanson, J. S. Tan, J. P. Rose, G. A. Voth, *J. Chem. Phys.* **2018**, *149*, 072310.
40. K. Pratt, W. Wakeham, *Proc. R. Soc. London, Ser. A* **1974**, *336*, 393-406.
41. A. J. Easteal, L. A. Woolf, *J. Phys. Chem.* **1985**, *89*, 1066-1069.
42. H. V. Ly, M. L. Longo, *Biophys. J.* **2004**, *87*, 1013-1033.
43. T.-X. Xiang, B. Anderson, *J. Membr. Biol.* **1994**, *140*, 111-122.
44. C. Zhu, L. Jiang, T.-M. Chen, K.-K. Hwang, *Eur. J. Med. Chem.* **2002**, *37*, 399-407.
45. G. Vizserálek, T. Balogh, K. Takács-Novák, B. Sinkó, *Eur. J. Pharm. Sci.* **2014**, *53*, 45-49.
46. N. Kučerka, S. Tristram-Nagle, J. F. Nagle, *J. Membr. Biol.* **2006**, *208*, 193-202.
47. W. Shinoda, *Biochim. Biophys. Acta, Biomembr.* **2016**, *1858*, 2254-2265.